Railway Sciences

Time-delay analysis between car body vertical acceleration and longitudinal track irregularity for EMUs

Wanru Xie
China Academy of Railway Sciences Corporation Limited, Infrastructure Inspection Research Institute, Beijing, China

Received 12 March 2026
Revised 8 June 2026
Accepted 5 July 2026

Abstract

Purpose – This paper aims to explore the time-delay mechanism between longitudinal track irregularity excitation and car body vertical acceleration of high-speed electric multiple units (EMUs). It addresses the existing research gap that previous studies mainly focus on vibration amplitude characteristics while ignoring the temporal transmission law of vehicle-track vibration.

Design/methodology/approach – This study combines theoretical modeling and measured data analysis. A mass-spring-damper vehicle dynamic model is established to clarify the delay generation mechanism during vibration transmission. Based on field inspection data, filtering and sliding window correlation analysis are adopted to compare vibration responses in bridge and subgrade sections. The Complete Ensemble Empirical Mode Decomposition with Adaptive Noise method is employed to extract the periodic irregularity component of 32 m simply supported beams, and the time delay is quantified through signal peak matching.

Findings – The suspension deformation of primary and secondary systems during vibration transmission is the essential cause of the time delay, which presents as a phase difference in the linear vehicle-track system. Owing to the periodicity of 32 m beam bridges, the track irregularity shows a higher correlation with car body acceleration (max correlation coefficient = 0.75) than subgrade sections. For typical high-speed EMUs, the stable time delay ranges from 0.4 s to 0.6 s, and the delay difference between the left and right tracks is extremely small (0–0.037 5 s).

Originality/value – This study systematically clarifies the physical mechanism of vibration transmission time delay in the vehicle-track system and develops a hybrid analysis method combining theoretical derivation and advanced signal processing. The quantified delay characteristics provide effective support for suspension parameter optimization, vibration model improvement and precise track maintenance of high-speed railways.

Keywords EMU, Longitudinal track irregularity, Car body vertical acceleration, Time delay, CEEMDAN, Vibration transmission

Paper type Research article

1. Introduction

With the continuous increase in the operating speed of electric multiple units (EMUs), the requirements for the smoothness and geometric quality of the track system have become increasingly stringent. When a train traverses the same track section at higher speeds, the amplitude of car body vibration increases significantly and the excited frequency band widens (Xie *et al.*, 2025a). To ensure operational safety, the amplitude of track geometric irregularities must be strictly controlled within acceptable limits. Currently, the maintenance rules for high-speed railway lines primarily adopt peak-value management to directly regulate the track geometric state, while utilizing vehicle dynamic responses, such as car body vertical and lateral accelerations, for auxiliary evaluation (Sun *et al.*, 2021; Xie *et al.*, 2024; Zhang, Li, Ling, & Zhai, 2025). The underlying principle of this auxiliary method is scientifically sound:

Funding: The financial support from the funds of National Natural Science Foundation of China (52308473) and China Academy of Railway Science Corporation Limited (2025YJ149) are gratefully acknowledged.

Railway Sciences
Emerald Publishing Limited
e-ISSN: 2755-0915
p-ISSN: 2755-0907
DOI 10.1108/RS-03-2026-0020

it treats the coupled track-vehicle system as an integrated entity. In this framework, the track geometric irregularity serves as the system input, the dynamic characteristics of the vehicle components (e.g. primary and secondary suspensions) act as the transfer function and the resulting car body vibration is the system output.

The primary goal of this auxiliary evaluation is to identify incipient defects in the track system by monitoring abnormal vibrations of EMUs during operation, thereby facilitating early risk warning (Xiao, Bai, Song, Sun, & Liu, 2024; Xie *et al.*, 2025; Xie *et al.*, 2025b). However, the vehicle system is inherently complex and highly nonlinear, making it challenging to develop an explicit, accurate analytical model for the aforementioned transfer function (Zhai, Stichel, & Ling, 2025; Chen *et al.*, 2024; An *et al.*, 2025). This limitation significantly curtails the practical value of the vehicle dynamic response-based evaluation method. A critical yet often overlooked factor is the time delay (or phase lag) between the track irregularity excitation and the car body vibration response. This delay arises from the dynamic characteristics of the spring-damper systems (e.g. primary and secondary suspensions), meaning the vehicle's dynamic response invariably lags behind the track irregularities that induce it. In time-domain signal analysis, this transmission phase difference manifests as a distinct time shift.

The presence of this time delay poses a significant challenge for practical maintenance. When abnormal car body vibrations are detected, frontline maintenance staff must rely on empirical judgment to pinpoint the corresponding location of the track irregularity before formulating a maintenance plan. This reliance on experience introduces a critical risk: an incorrect localization of the anomalous track section can lead to ineffective maintenance plans, allowing potential operational hazards to persist. Therefore, a precise analysis and quantification of the time delay characteristics between track geometric irregularities and vehicle dynamic responses are imperative. This effort is crucial for advancing the auxiliary track evaluation method from its current state of empirical judgment towards intelligent, data-driven diagnosis.

Concurrently, the rapid development of deep learning and artificial intelligence technologies has spurred their application within the railway industry, making it a burgeoning research hotspot. Several studies have explored predicting car body acceleration based on track geometry data (Ma, Liu, Zhang, Chen, & Zhao, 2023; He, Li, Li, Wang, & Wang, 2023; Zhao *et al.*, 2026). These works consistently highlight that the selection and preprocessing of training data profoundly impact model accuracy. For instance, Zhao *et al.* (2026) emphasized the necessity of using sufficiently long data segments to compensate for system errors caused by the hysteresis effect of the suspensions. It is evident that efficiently and accurately determining the time delay between the track state and the vehicle system's response is a key scientific issue that must be resolved to enable the development of reliable digital twin technology for high-speed railways. While these data-driven methods show great promise, a precise physical understanding of the time delay mechanism remains the fundamental bedrock for improving their accuracy, robustness and interpretability.

In view of the above research gap and practical demand, this study aims to thoroughly investigate the time delay mechanism between longitudinal track irregularity and car body vertical acceleration of EMUs. Through theoretical derivation based on a mass-spring-damper model, we first clarify that the time delay originates from the finite deformation time required during the force transmission process of the primary and secondary suspension systems. Subsequently, we propose an integrated methodology combining theoretical analysis, advanced signal processing, and verification with measured data from high-speed comprehensive inspection trains. This methodology employs sliding window correlation analysis to reveal the characteristic differences in the correlation between excitation and response under different track substructures (bridges vs subgrades). Innovatively, the Complete Ensemble Empirical Mode Decomposition with Adaptive Noise (CEEMDAN) technique is applied to extract the single periodic component induced by 32 m simply supported beams from the complex longitudinal track irregularity signals, thereby achieving an accurate quantification of the time delay range for a typical EMU.

The remainder of this paper is organized as follows. Section 2 details the theoretical analysis of the time delay mechanism. Section 3 describes the signal modeling and the calculation method. Section 4 analyzes the characteristics of track irregularities and their correlation with car body acceleration. Section 5 presents the application and results based on measured data. Finally, Section 6 concludes the paper.

2. Theoretical analysis of time delay mechanism

2.1 Simplified model of the vehicle-track system

Theoretically, any mechanical system can be modeled as a mass-spring-damper vibration system. Therefore, the forced vibration components of railway vehicles (car body, bogie and wheelset) and the connecting suspension devices (primary and secondary suspensions) are simplified into a mass-spring-damper system, as shown in Figure 1. According to mechanical vibration theory, when an external excitation acts on the system, the dynamic equation can be expressed as Equation (1):

$$\boldsymbol{M}\ddot{x} + \boldsymbol{C}\dot{x} + \boldsymbol{K}x = \boldsymbol{F} \tag{1}$$

where M is the mass matrix of the vibration system; C is the damping matrix; K is the stiffness matrix; x is the system response vector and F is the external excitation matrix.

2.2 Definition and characteristics of longitudinal track irregularity

The wheelsets of EMUs are in direct contact with the rails of the track system. Under ideal conditions, the wheelsets roll on the rails. However, due to the existence of longitudinal track irregularity, the wheelsets exhibit "follow-up" motion in the horizontal plane in response to changes in track elevation during rolling.

The rule for defining longitudinal track irregularity is as follows: if the longitudinal track profile is lower than the designed longitudinal profile, the irregularity is taken as negative; if it is higher, the irregularity is taken as positive, as illustrated in Figure 2 (the dashed line represents the designed longitudinal profile of the line).

2.3 Transmission path of force and vibration

When the EMU continues to operate (as shown in Figure 2), the positive-amplitude longitudinal track irregularity induces a vertical acceleration of the wheelset along the positive z-axis. As the right wheel generates acceleration and displaces along the z-axis, the primary suspension spring connected to the bogie contracts, exerting an upward vertical force on the bogie. Similarly, the left wheel applies a force to the bogie under the influence of longitudinal

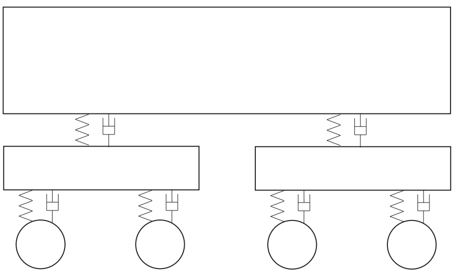

Figure 1. Simplified schematic diagram of a high-speed EMU. **Source(s):** Author's own work

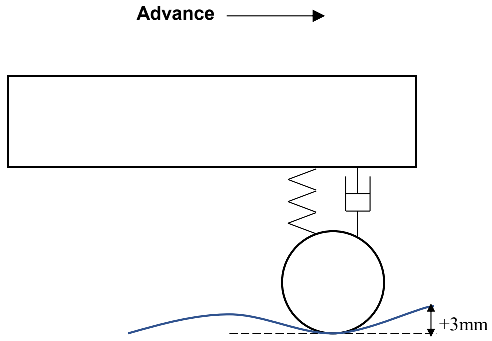

Figure 2. Schematic diagram of track longitudinal irregularity. **Source(s):** Author's own work

track irregularity. For the same bogie, forces from two wheelsets (four wheel sides) are superimposed, resulting in vibrational acceleration that can be decomposed into lateral and vertical components.

In the horizontal plane, the vertical vibrational acceleration of the bogie causes deformation of the secondary suspension springs connected to the car body, thereby generating a vertical force acting on the car body. The combined effect of the front and rear bogies induces vertical acceleration of the car body. From a physical perspective, acceleration can change instantaneously, whereas force cannot, spring deformation requires a certain amount of time. Consequently, a time interval exists between longitudinal track irregularity and the resulting car body vertical acceleration, which is directly related to the characteristics of the primary and secondary suspension springs.

Figure 3 illustrates the EMU operating under positive-amplitude longitudinal track irregularity. At this point, the wheelset follows the irregularity and displaces toward the positive z-axis in the horizontal plane, generating an upward acceleration a_{wheelset}. The upward displacement of the wheelset compresses the primary suspension spring, applying a force on the bogie along the positive z-axis.

Similarly, the bogie is also subjected to a force F′ from the other wheelset. If the resultant direction of F and F' is upward, the bogie will generate a vertical acceleration a_{bogie} under the action of the external force ($F + F'$). The magnitude and direction of F' depend on the longitudinal track irregularity contacted by the other wheelset. The force-bearing state of the bogie is shown in Figure 4.

The force transfer between the bogie and the car body via the secondary suspension spring is similar to that of the primary suspension spring. Assuming the resultant force on the bogie (as shown in Figure 4) is along the positive z-axis, the force analysis between the bogie and the car body is presented in Figure 5. When the bogie is subjected to an upward resultant force along the z-axis, it generates an upward vertical acceleration a_{bogie} and displaces upward,

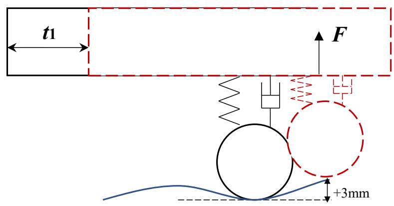

Figure 3. Force analysis of the wheelset-bogie system. **Source(s):** Author's own work

Figure 4. Schematic diagram of bogie force distribution. **Source(s):** Author's own work

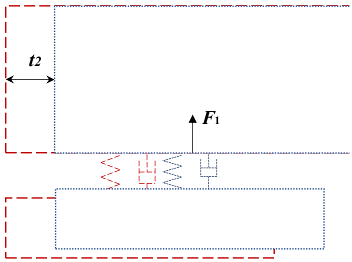

Figure 5. Force analysis of the bogie-car body system. **Source(s):** Author's own work

compressing the secondary suspension spring and applying an upward force on the car body along the positive z-axis.

Similarly, the car body is subjected to a force F_2 from the other bogie. If the resultant direction of F_1 and F_2 is upward, the car body will generate a vertical acceleration a_{carbody} under the action of the external force $(F_1 + F_2)$. The force-bearing state of the car body is shown in Figure 6.

Based on the force and motion transmission relationship, the time interval between longitudinal track irregularity and the resulting car body vertical acceleration is the sum of t_1 (transmission time through the primary suspension, as shown in Figure 3) and t_2 (transmission time through the secondary suspension, as shown in Figure 5).

3. Time delay calculation method based on vibration transmission

3.1 System signal modeling

Calculating the time delay between longitudinal track irregularity and car body vertical acceleration is equivalent to solving the sum of t_1 and t_2 described above. In this process, longitudinal track irregularity can be regarded as the input signal, car body vertical acceleration as the output signal and the characteristics of the primary and secondary suspension springs as the transfer function.

As a complex nonlinear mechanical structure, EMUs have multiple natural modes in each component. When vibrations generated at the wheel-rail interface are transmitted step by step to the bogie and car body via the primary and secondary suspension springs, resonance may occur if the vibration frequency is close to the natural frequency of the car body or bogie. That is, at the same operating speed, EMUs exhibit different sensitivities to track geometric irregularities of different wavelengths.

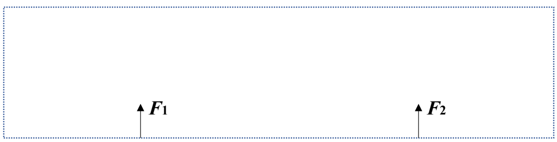

Figure 6. Schematic diagram of car body force distribution. **Source(s):** Author's own work

3.2 Derivation of core theoretical formulas

Wang, Liu, and Liang (2009) proposed a *Generalized Energy Index (GEI)* for comprehensively evaluating the dynamic characteristics of the vehicle-track system, which uses weight coefficients to characterize the vehicle vibration characteristics induced by irregularities of different wavelengths. The *GEI* is calculated as Equation (2):

$$GEI = \sum_{i=1}^{7} \alpha_i \sqrt{\frac{1}{n-1} \sum_{j=0}^{n-1} \omega(f_j) E_i(f_j)} \tag{2}$$

where α_i is the pre-given weight coefficient of the i-th single index; $E_i(f_j)$ is the energy of the i-th single irregularity corresponding to wavelength f_j and $\omega_i(f_j)$ is the energy weight coefficient corresponding to wavelength f_j.

The energy weight coefficient $\omega_i(f_i)$ must satisfy the following normalization condition in Equation (3):

$$\sum_{j=0}^{n-1} \omega(f_j) = 1 \tag{3}$$

The *GEI* indicates that different wavelength components of irregularities contribute differently to carbody vibration, and these contributions are independent and quantifiable.

Through Fourier transform, the time-domain longitudinal track irregularity can be converted into a frequency-domain signal shown in Equation (4):

$$Y(f) = \int_0^L y(t) e^{-j2\pi ft} dt \tag{4}$$

where $Y(f)$ is the frequency-domain expression of longitudinal track irregularity; $y(t)$ is the time-domain expression of longitudinal track irregularity and L is the total length of the signal.

When the longitudinal track irregularity has a unique wavelength and fixed amplitude, the car body vertical acceleration generated by the EMU is also uniquely determined. Ignoring other factors affecting car body vibration except track geometric irregularity, the longitudinal track irregularity contains complex wavelength components and the car body vertical acceleration can be expressed as Equation (5):

$$A(f) = \sum H_i \cdot Y_i(f) \tag{5}$$

where $A(f)$ is the Fourier transform of car body vertical acceleration; H_i is the transfer coefficient corresponding to the i-th wavelength component signal and $Y_i(f)$ is the functional expression corresponding to the i-th wavelength component.

The transfer coefficient H_i in Equation (5) has the same physical meaning as the energy weight coefficient $\omega_i(f_i)$ corresponding to wavelength f_i in the *GEI* calculation formula, reflecting the sensitivity of the car body to the irregularity component of wavelength f_i. A larger H_i indicates that this wavelength induces a more significant change in car body vertical acceleration compared to other track geometric irregularities of the same amplitude.

Assuming the longitudinal track irregularity has a single unique wavelength, Equation (5) simplifies to Equation (6):

$$A(f) = H \times Y(f) \tag{6}$$

Since $Y(f)$ is a periodic signal (assumed to be a sine function), its time-domain can be expressed as Equation (7):

$$y(t) = \sin(2\pi f \times t) \tag{7}$$

Due to the existence of time delay, the quantitative relationship between car body vertical acceleration and longitudinal track irregularity in the time domain can be expressed as Equation (8):

$$a(t+\tau) = h * \sin(2\pi f \times t) \tag{8}$$

where τ is the time delay between car body vertical acceleration induced by longitudinal track irregularity and the corresponding longitudinal track irregularity; h is the value of the transfer function corresponding to the frequency f, which is a constant; * denotes the convolution operation.

When the wavelength λ of longitudinal track irregularity is determined, the relationship between signal frequency f and train operating speed v is defined as Equation (9):

$$f = \frac{v}{\lambda} \tag{9}$$

Combined with the above formula, the quantitative relationship between operating speed and time delay is expressed as Equation (10). It can be found that different running speeds will lead to variations of frequency f, while the time delay τ remains unchanged and is not affected by the operating speed.

$$a(t+\tau) = h * \sin\left(2\pi \frac{v}{\lambda} \times t\right) \tag{10}$$

3.3 Key procedures for time delay calculation

Based on the above analysis, the key to calculating the time delay between car body vertical acceleration and longitudinal track irregularity is to identify track sections with single-component vertical irregularity. If some track segments with a single component of vertical irregularity can be obtained, the time-delay calculation can be quantified by the following steps:

(1) Identify the starting point of single-component longitudinal track irregularity and the corresponding starting point of carbody vertical acceleration change;

(2) Extract time information of peak points of periodic longitudinal track irregularity;

(3) Extract time information of peak points of corresponding car body vertical acceleration and

(4) Calculate the difference between the two sets of time information, which is the time delay between car body vertical acceleration and longitudinal track irregularity.

4. Characteristic analysis of longitudinal track irregularity

4.1 Data acquisition and preprocessing

Currently, high-speed comprehensive inspection trains are equipped with acceleration sensors and string displacement meters at the car body to collect longitudinal track irregularity data $Y(x)$ and car body vertical acceleration data $A(x)$ during operation, which are used to evaluate the track geometric state of the section.

The collected data are one-dimensional sequence data under spatial sampling, including the amplitude of longitudinal track irregularity and car body vertical acceleration at the current position, with a sampling frequency of four points per meter. Figures 7 and 8 show the original

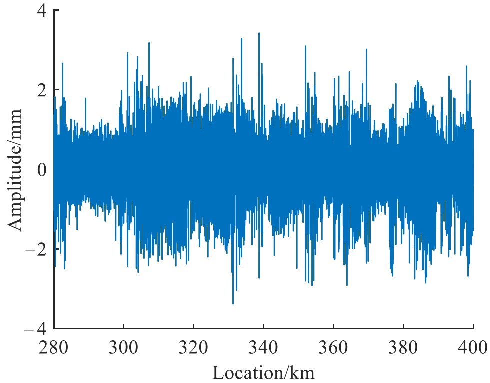

Figure 7. Left-track longitudinal irregularity. **Source(s):** Author's own work

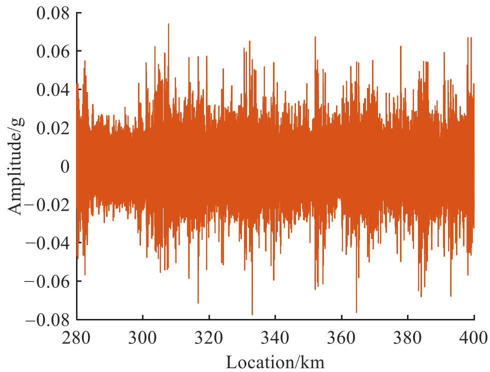

Figure 8. Carbody vertical acceleration. **Source(s):** Author's own work

waveforms of left longitudinal track irregularity and car body vertical acceleration of a typical line.

As shown in the figures, the amplitude of left longitudinal track irregularity ranges from −3.5 mm to 3.5 mm, and the amplitude of car body vertical acceleration ranges from −0.07 g to 0.06 g. There are differences in dimensions and amplitudes between the 2 datasets.

Based on this, the data preprocessing process is as follows:

(1) Remove data from low-speed operation sections and acceleration/deceleration sections.

(2) Filter the signal with a frequency band of [0, 1/30×Fs] to retain track irregularity components with wavelengths greater than 30 m. The selection of the 30 m cutoff wavelength follows the standard wavelength classification of high-speed railway track irregularities and the vertical vibration sensitive characteristics of high-speed EMUs. In actual high-speed railway lines, medium and high-frequency periodic interference signals are widely generated by track welds, track plate structures and short-wave micro-irregularities, which belong to local high-frequency disturbances and cannot induce overall car body vertical vibration. The adopted 30 m wavelength threshold can effectively filter out the above irrelevant medium and high-frequency interference components. Meanwhile, it completely reserves the low-frequency

periodic irregularity characteristics induced by 32 m simply supported beams, which are the dominant excitation source triggering synchronous car body vertical vibration. This filtering strategy ensures that the extracted vibration signals are highly matched with the research object of beam-induced vibration transmission delay, guaranteeing the pertinence and accuracy of subsequent time-delay quantification.

(3) Normalize the longitudinal track irregularity and car body vertical acceleration data using min-max normalization to map the values to the interval [0, 1], as shown in Equation (11)

$$X_{norm} = \frac{X - \min(X)}{\max(X) - \min(X)} \tag{11}$$

where X is the original dataset; max(X) is the maximum value in the dataset and min(X) is the minimum value in the dataset.

A sliding window method with a step size of 20 m and a section length of 500 m is used for data segmentation, resulting in 5,967 data segments. Taking the left rail as an example, the correlation coefficient between the normalized longitudinal track irregularity and car body vertical acceleration is calculated using Equation (12). The section length of 500 m is chosen to weaken the loss of correlation coefficient caused by time delay with a sufficiently long signal.

$$\rho_{xy} = \frac{\sum\left[\left(x_i - \bar{x}\right)\left(y_i - \bar{y}\right)\right]}{\sqrt{\sum\left(x_i - \bar{x}\right)^2 \times \sum\left(y_i - \bar{y}\right)^2}} \tag{12}$$

Where x_i is the i-th sample value of the normalized longitudinal track irregularity and y_i is the corresponding value of the car body vertical acceleration.

4.2 Correlation analysis between longitudinal track irregularity and car body acceleration

The absolute values of the correlation coefficients between left longitudinal track irregularity and car body vertical acceleration for 5,967 sections are calculated, and their cumulative distribution is plotted, as shown in Figure 9. Figure 9 presents the correlation coefficients corresponding to different cumulative probabilities.

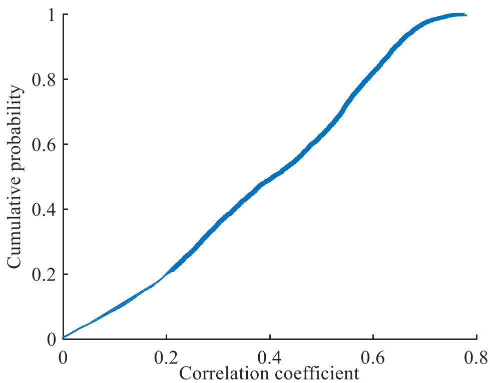

Figure 9. Cumulative distribution of absolute correlation coefficients between track longitudinal irregularity and car body vertical acceleration. **Source(s):** Author's own work

The results in Figure 9 indicate that the absolute values of the correlation coefficients vary among different sections, mainly affected by the wavelength and shape of longitudinal track irregularity. The maximum absolute correlation coefficient is 0.7783, indicating a strong correlation between left longitudinal track irregularity and car body vertical acceleration. For 50% of the sections, the absolute correlation coefficient is less than 0.41, suggesting a weak but existent relationship between longitudinal track irregularity and car body vertical vibration. However, in actual operation, the vibration transmission process suffers from a certain loss rate due to the vibration isolation effect of the primary and secondary suspension springs and the state of the car body itself.

One section is selected for each absolute correlation coefficient of 0.2, 0.4, 0.6 and 0.75 between left longitudinal track irregularity and car body vertical acceleration, and the original waveforms are plotted, as shown in Figures 10–13.

As shown in Figures 10–13, when the absolute correlation coefficient is 0.2, the left longitudinal track irregularity exhibits obvious random characteristics. With the increase in the correlation coefficient, the periodicity of left longitudinal track irregularity gradually becomes significant. Figure 13(a) is located in a bridge section, where the periodicity of left longitudinal track irregularity corresponds to the 32 m simply supported beam. At this point, the car body vertical acceleration also shows a similar periodic characteristic, indicating that the periodic longitudinal track irregularity induced by the 32 m simply supported beam has a significant excitation effect on car body vertical vibration.

4.3 Analysis of correlation characteristics under different track substructures

In total, 17 sections with an absolute correlation coefficient greater than 0.75 are identified, and all of these sections correspond to bridge substructures. According to the account information, all strongly correlated sections correspond to bridge substructures.

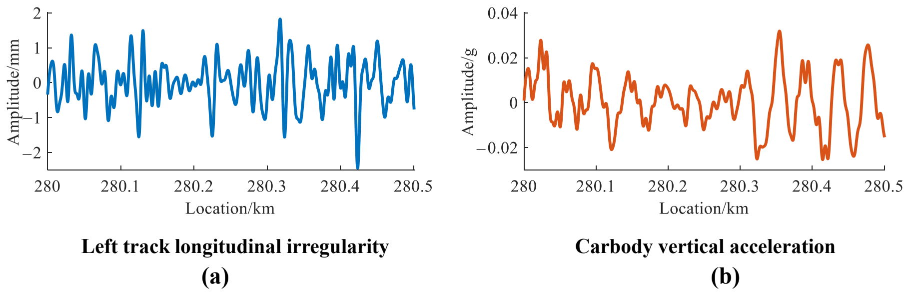

Figure 10. Absolute correlation coefficient = 0.2. **Source(s):** Author's own work

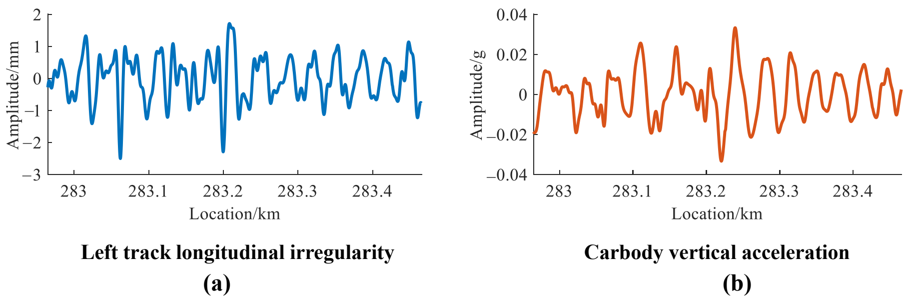

Figure 11. Absolute correlation coefficient = 0.4. **Source(s):** Author's own work

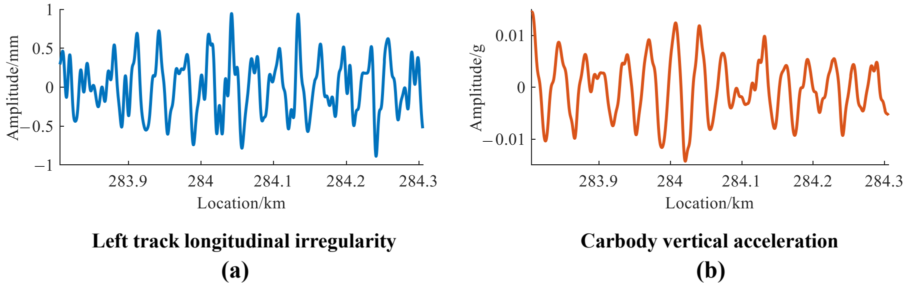

Figure 12. Absolute correlation coefficient = 0.6. **Source(s):** Author's own work

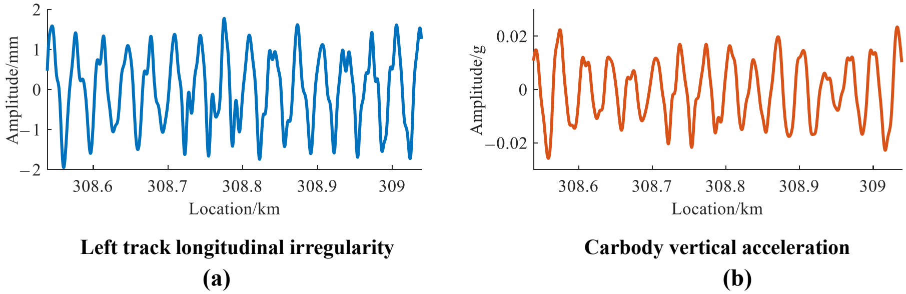

Figure 13. Absolute correlation coefficient = 0.75. **Source(s):** Author's own work

According to the account information, there are no tunnel sections in the current line. A 500 m section completely located on a bridge is defined as a bridge section; a section partially on a bridge and partially on a subgrade is not recorded; and a section completely located on a subgrade is defined as a subgrade section. Based on this definition, a total of 3,730 bridge sections and 1,075 subgrade sections were identified from the dataset.

The cumulative distribution curves of the absolute correlation coefficients between left longitudinal track irregularity and car body vertical acceleration for bridge and subgrade sections are plotted, as shown in Figure 14. It can be seen that the cumulative distribution curve of bridge sections is located to the right of that of subgrade sections, indicating that the correlation between longitudinal track irregularity and car body vertical acceleration in bridge sections is significantly higher than that in subgrade sections. That is, the influence of longitudinal track irregularity on car body vertical acceleration in bridge sections is greater than that in subgrade sections.

Figure 15 compares the absolute correlation coefficients between left and right longitudinal track irregularity and car body vertical acceleration. The results show that the difference between the absolute correlation coefficients of left and right rails is small.

5. Time-delay calculation application based on measured data

5.1 Selection of measured data

The analysis above indicates that when the EMU travels on bridge sections, the longitudinal track irregularity exhibits periodic characteristics due to the 32 m simply supported beams, which well meets the requirement of single-component longitudinal track irregularity for time-delay calculation. According to Figure 13, when the EMU operates stably on bridges, both the longitudinal track irregularity and car body vertical acceleration show significant periodic characteristics, verifying the rationality of Equation (6). However, it is difficult to determine the correspondence between longitudinal track irregularity and car body vertical acceleration in such cases.

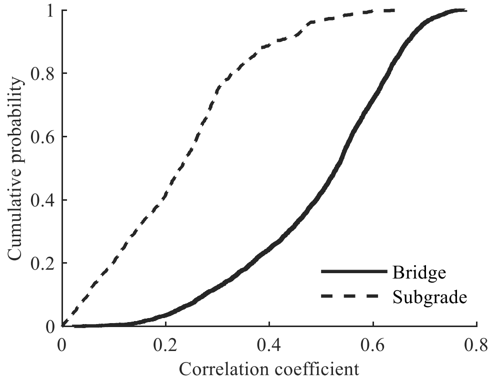

Figure 14. Cumulative distribution curves of absolute correlation coefficients for different track substructures. **Source(s):** Author's own work

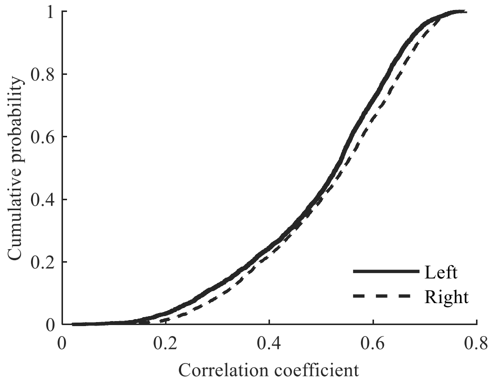

Figure 15. Cumulative distribution curves of absolute correlation coefficients for left- and right-track longitudinal irregularity. **Source(s):** Author's own work

Therefore, data from the section shown in Figure 16 are selected for analysis, and the corresponding car body vertical acceleration is presented in Figure 17.

As shown in Figures 16 and 17, there is a good correspondence between left and right longitudinal track irregularity and car body vertical acceleration in this section. Near 329.700

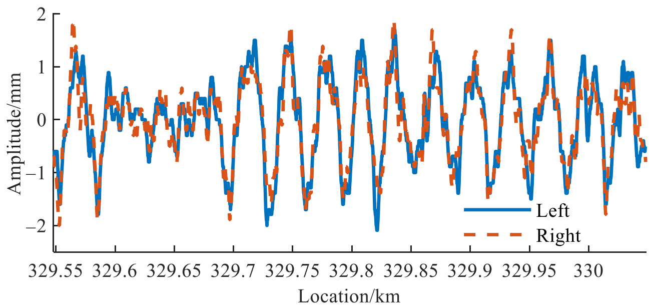

Figure 16. Original waveforms of left- and right-track longitudinal irregularity. **Source(s):** Author's own work

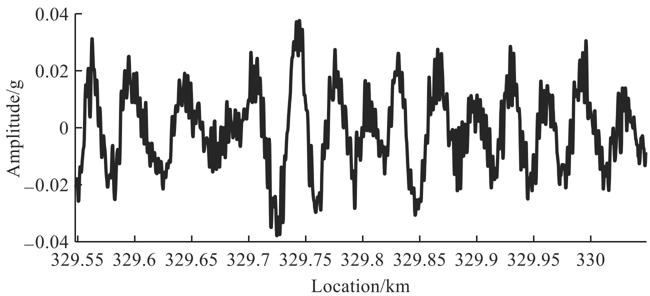

Figure 17. Original waveform of carbody vertical acceleration. **Source(s):** Author's own work

kilometers, the car body vertical acceleration can be clearly observed to change with the longitudinal track irregularity, satisfying the time-delay calculation conditions: (1) single-component longitudinal track irregularity with a clear starting point and (2) longitudinal track irregularity changes induce car body vertical acceleration changes with a clear starting point.

5.2 Signal decomposition and single-component extraction

As shown in Figure 16, the longitudinal track irregularity data contain components of other wavelengths in addition to the 32 m periodic simply supported beam component. Direct application of the time-delay calculation method to the original data will result in large errors. Therefore, the longitudinal track irregularity and car body vertical acceleration signals are preprocessed to extract single components.

Following the steps in Xie *et al.* (2025c), the left/right longitudinal track irregularity and car body vertical acceleration data are decomposed using the CEEMDAN (Torres, Colominas, Schlotthauer, & Flandrin, 2011), a method extended from the original Ensemble Empirical Mode Decomposition (Wu & Huang, 2009). The total number of added noise iterations N is set to 100, and the signal-to-noise ratio ε_0 is set to 0.2.

After CEEMDAN decomposition, K intrinsic mode functions (IMFs) with different frequencies and one residual term are obtained, expressed as Equation (13):

$$D(x) = \sum_{i=1}^{K} C_i(x) + R(x) \tag{13}$$

where $D(x)$ is the original signal; $C_i(x)$ is the i-th decomposed IMF; $R(x)$ is the residual term and K is the total number of IMFs.

After CEEMDAN, the left/right longitudinal track irregularity and car body vertical acceleration data shown in Figures 16 and 17 are each decomposed into 9 IMFs and 1 residual term. The root mean square (RMS) value reflects the energy of the signal–the larger the RMS value, the greater the energy of the current IMF and the more information it carries from the original signal. In bridge sections, due to the existence of 32 m simply supported beams, the longitudinal track irregularity is dominated by the 32 m wavelength component. Therefore, the RMS value of each IMF is calculated using Equation (14), and the IMF with the largest RMS value (denoted as C_{m}) is extracted, which is the desired single-component longitudinal track irregularity signal.

$$RMS(C_i) = \sqrt{\frac{1}{M}\sum_{j=1}^{M} C_i(j)^2}, i = 1, 2, \ldots, K \tag{14}$$

where C_i is the i-th IMF decomposed by CEEMDAN; K is the total number of decomposed IMFs; M is the signal length and j is the current data point index.

Figure 18 compares the left longitudinal track irregularity C_m obtained by CEEMDAN with the original signal. It can be seen that C_m effectively retains the periodic component of vertical irregularity corresponding to the 32 m simply supported beam while suppressing interference components of other wavelengths, verifying the scientificity and effectiveness of CEEMDAN for data processing.

Figure 19 shows the C_m waveforms of left and right longitudinal track irregularity.

Comparing Figures 18 and 19, it can be seen that the 32 m periodic vertical irregularity component at the position of the black rectangular box in these figures will cause the vertical vibration of the vehicle body to intensify. Before the dashed box, the longitudinal track irregularity has no obvious periodicity and small amplitude, and the corresponding car body vertical acceleration also has no obvious periodicity and small amplitude. Within the dashed box, the longitudinal track irregularity exhibits periodic characteristics with significantly increased amplitude, and the corresponding car body vertical acceleration also shows periodicity with increased amplitude. Based on this, it is determined that the peak point ① of vertical irregularity in Figure 19 corresponds to the peak point ① of car body vertical acceleration in Figure 18.

5.3 Peak matching and time-delay calculation

Taking the arrow-marked peak point ① in Figure 19 as the first peak, the mileage information of peak points of left/right longitudinal track irregularity is extracted: from 329.690 to 330.048 kilometers, both left and right longitudinal track irregularity contain 22 peak points. Taking the arrow-marked peak point ① in Figure 18 as the first peak, the mileage information of peak

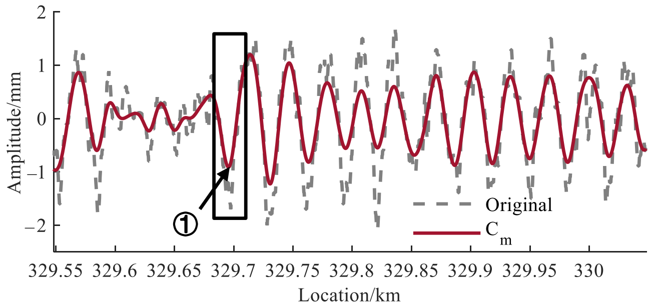

Figure 18. Comparison between left-track longitudinal irregularity C_m and the original signal. **Source(s):** Author's own work

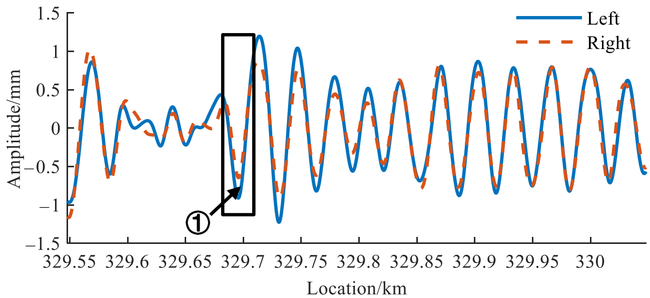

Figure 19. C_m of left and right-track longitudinal irregularity. **Source(s):** Author's own work

points of car body vertical acceleration is extracted: from 329.710 to 330.048 kilometers, the car body vertical acceleration data contains 20 peak points.

The EMU operates at an approximately constant speed of 192 km/h through this section. Based on the correspondence, the mileage of peak points of left/right longitudinal track irregularity and the corresponding car body vertical acceleration is plotted, as shown in Figure 20.

As shown in Figure 20, the mileage difference between peak points of the same sequence of left and right longitudinal track irregularity is very small – the maximum mileage difference is 1.5 m and the minimum is 0 m. Combined with the C_m waveform characteristics of left and right longitudinal track irregularity in Figure 19, it can be concluded that the left and right longitudinal track irregularity in this section have good consistency.

Notably, although the train will inevitably produce slight rolling motion during operation, the rolling response is mainly excited by the differential component of bilateral track irregularity excitation. For the standard 32 m simply supported beam bridge adopted in high-speed railways, the overall deformation of the bridge deck is uniform, leading to nearly synchronous and symmetric excitation input on the left and right rails. The car body center-of-mass vertical acceleration is dominantly determined by the superposition of symmetric vertical vibration responses of the left and right suspension systems, while the asymmetric rolling motion only produces minor secondary coupling interference, which hardly changes the vibration transmission phase and response lag of the main vertical vibration.

In addition, the corresponding mileage of peak points shows a roughly linear increasing trend, indicating that the distance between adjacent peak points is basically the same, meaning the C_m of left and right longitudinal track irregularity have strong periodicity. The distance between adjacent peak points ranges from 13.25 m to 20.05 m, and the frequency of different interval distances is shown in Figure 21. Among them, the interval distance between adjacent

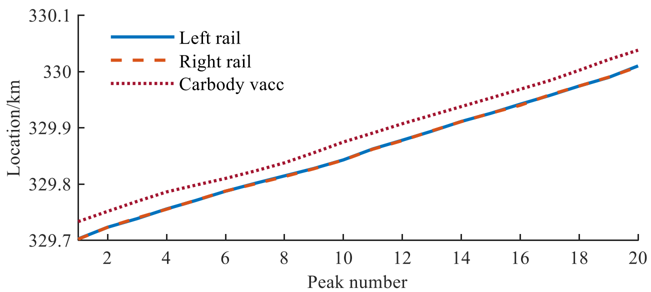

Figure 20. Corresponding mileage of peak points of left-/right-track longitudinal irregularity and car body vertical acceleration. **Source(s):** Author's own work

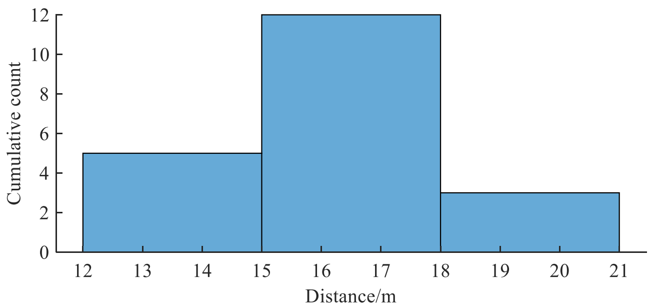

Figure 21. Frequency histogram of different interval distances. **Source(s):** Author's own work

peak points falls within the range of 15–18 m 12 times, accounting for 60%, which is very close to half the length of the 32 m simply supported beam.

After calculating the interval distance between peak points of left and right longitudinal track irregularity and the corresponding car body vertical acceleration, the time delay is calculated based on the operating speed, as shown in Figure 22.

As shown in Figure 22, taking the peak sequence of the left longitudinal track irregularity as the reference, the time delay between car body vertical acceleration and left-track irregularity ranges from 0.412 5 s to 0.595 3 s. Taking the peak sequence of the right longitudinal track irregularity as the reference, the time delay ranges from 0.421 8 s to 0.600 s. For the identical car body vertical acceleration peak, the time-delay difference calculated based on left- and right-track excitations is only within 0–0.037 5 s, which is negligible.

The extremely small bilateral time-delay difference further confirms that the symmetric track excitation of the simply supported beam bridge dominates the vehicle vertical vibration response, and the minor rolling motion has no substantial influence on the vibration transmission time delay. In summary, the stable vibration transmission time delay between longitudinal track irregularity and car body vertical acceleration of typical high-speed EMUs is determined to range from 0.4 s to 0.6 s under conventional steady-speed operating conditions on 32 m simply supported beam bridge sections.

6. Conclusions

This study investigates the time-delay characteristics between car body vertical acceleration and longitudinal track irregularity for high-speed EMUs and proposes a data-driven time-delay calculation method based on theoretical derivation and field measured data. The stable time delay range of a typical high-speed EMU is quantitatively identified, and the main conclusions are summarized as follows:

(1) The essential mechanism of the vibration transmission time delay is clarified via force analysis. Track irregularity-induced wheelset vertical acceleration changes instantaneously, whereas structural force transmission exhibits temporal hysteresis. The excitation generated by longitudinal track irregularity requires a certain duration to be converted into elastic forces of primary and secondary suspensions and further transmitted to the car body through the bogie, forming a stable vibration transmission time delay.

(2) Under the premise of excluding interference from non-track vibration factors, the coupling system of longitudinal track irregularity and car body vertical acceleration can be regarded as a superposition of multiple linear time-invariant systems. For periodic track irregularity signals, the time delay of vehicle vibration transmission can

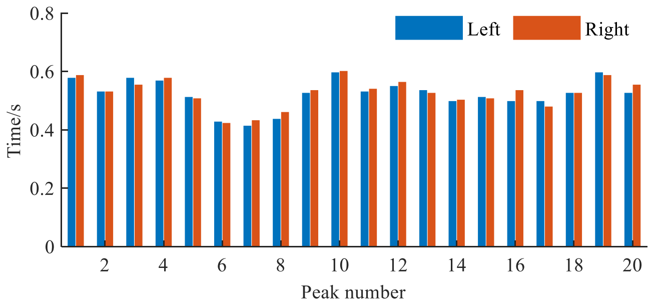

Figure 22. Time delay calculated from different peak points in this section. **Source(s):** Author's own work

be equivalently determined by calculating the phase difference between track irregularity and car body vertical acceleration sequences.

(3) Compared with subgrade sections, track irregularities on bridge sections present a significantly higher correlation with car body vertical acceleration. This is mainly attributed to the prominent periodic excitation characteristics formed by 32 m simply supported beams, which provide stable and coherent vibration input. The maximum correlation coefficient reaches 0.75 for periodic bridge track sections. In addition, the left and right rails yield consistent correlation results within the same line section, indicating uniform vertical vibration responses of the vehicle to bilateral track excitations.

(4) Based on CEEMDAN-processed measured signals of typical bridge sections, the time-delay difference between left-track- and right-track-induced car body vertical acceleration is negligible for typical high-speed EMUs. The overall stable vibration transmission time delay range of the typical high-speed EMU is determined to be 0.4–0.6 s.

7. Applicable conditions, limitations and future prospects

The data-driven method proposed in this study avoids the dependence on confidential vehicle suspension stiffness and damping parameters required by traditional mechanism-driven models and only relies on field-measured track-and-vehicle vibration data, which possesses good engineering practicability and universality. The identified 0.4–0.6 s time-delay range is applicable to typical high-speed EMUs operating at steady uniform speed on high-speed railway 32 m simply supported beam bridge sections. The vibration transmission time delay investigated in this study is an inherent structural response lag of the vehicle suspension system, which is insensitive to minor steady-speed variations.

This study still has several limitations. First, this paper adopts a linear time-invariant system assumption to extract the dominant time-delay law of vibration transmission, which simplifies the weak nonlinear damping characteristics of actual suspension components. Second, restricted by the confidentiality of vehicle core parameters, parametric sensitivity analysis of suspension stiffness and damping is not carried out. Third, the research results are obtained based on typical bridge and single-speed working conditions; the time-delay variation characteristics under different EMU platforms, operating speeds and line types are not comprehensively compared and analyzed.

On this basis, future research will be expanded from two aspects. First, through cooperation with vehicle manufacturers, authorized confidential vehicle parameters and numerical simulation methods will be adopted to carry out parametric sensitivity analysis, and the nonlinear dynamic characteristics of suspension will be considered in refined modeling to further supplement the physical mechanism of vibration transmission delay. Second, relying on the good universality of the proposed data-driven method, multi-condition measured data of different EMU types, various operating speeds and diverse line structures will be collected to systematically enrich the time-delay characteristic database, summarize the time-delay evolution rules under different working conditions and further improve the theoretical system of vehicle-track-coupled vibration transmission for high-speed railways.

References

An, B., Liu, J., Yang, G., Liu, F., Shi, T., & Zhai, M. (2025). Parameter influence analysis and optimization of wheel-rail creepage characteristics in high-speed railway curves. *Railway Sciences*, *4*(1), 37–51. doi: 10.1108/rs-12-2024-0056.

Chen, Z., Ning, J., Yang, G., Chen, Z., Yang, J., & Zhai, W. (2024). Dynamic characteristics of rack vehicle-track coupled system on large slope line: Theoretical modelling and experimental validation. *Vehicle System Dynamics*, *62*(9), 2304–2331. doi: 10.1080/00423114.2023.2282717.

He, Q., Li, L., Li, C., Wang, J., & Wang, P. (2023). A mapping model between track irregularity and vertical car-body acceleration based on deep learning. *Journal of the China Railway Society*, *45* (6), 106–113.

Ma, S., Liu, X., Zhang, Y., Chen, Z., & Zhao, D. (2023). Track geometry state assessment method for high-speed railway based on vehicle response. *Journal of the China Railway Society*, *45*(11), 117–127.

Sun, J., Meli, E., Cai, W., Gao, H., Chi, M., Rindi, A., & Liang, S. (2021). A signal analysis based hunting instability detection methodology for high-speed railway vehicles. *Vehicle System Dynamics*, *59*(10), 1461–1483. doi: 10.1080/00423114.2020.1763407.

Torres, M. E., Colominas, M. A., Schlotthauer, G., & Flandrin, P. (2011). A complete ensemble empirical mode decomposition with adaptive noise. In *2011 IEEE International Conference on Acoustics, Speech and Signal Processing (ICASSP)*, New York (pp. 4144–4147). IEEE Press.

Wang, W., Liu, J., & Liang, Z. (2009). Generalized energy index for comprehensively evaluating the dynamic characteristics of vehicle/track system. *China Railway Science*, *30*(5), 22–27.

Wu, Z., & Huang, N. E. (2009). Ensemble empirical mode decomposition: A noise-assisted data analysis method. *Advances in Adaptive Data Analysis*, *1*(1), 1–41. doi: 10.1142/s1793536909000047.

Xiao, J., Bai, Y., Song, C., Sun, S., & Liu, X. (2024). Feature analysis of precipitation-induced subgrade defects on a high-speed rail ballasted track using multiple track inspection data: A case study. In *Proceedings of the Institution of Mechanical Engineers, Part F: Journal of Rail and Rapid Transit*, *238*(7), 837–850. doi: 10.1177/09544097241234094.

Xie, W., Liu, J., Zhao, G., Sun, L., Xiao, X., & Zhang, M. (2024). Time frequency characteristic analysis and fast diagnosis method of low frequency periodic vehicle body hunting. *Journal of Mechanical Engineering*, *60*(18), 318–326.

Xie, Q., Peng, F., Tao, G., Ren, Y., Liu, F., Yang, J., & Wen, Z. (2025). Monitoring track irregularities using multi-source on-board measurement data. *Railway Engineering Science*, *33*(4), 746–765. doi: 10.1007/s40534-024-00374-0.

Xie, W., Zhao, Y., Zhao, G., Yang, F., Qin, H., & Wei, Z. (2025a). Analysis of frequency domain characteristics for hunting of high-speed EMUs in turnout area. *Journal of the China Railway Society*, *47*(4), 41–50.

Xie, W., Zhao, Y., Zhao, G., Yang, F., Wei, Z., & Liu, J. (2025b). Research on the rapid diagnosis method for hunting of high-speed trains. *Railway Sciences*, *4*(1), 1–21. doi: 10.1108/rs-10-2024-0042.

Xie, W., Liu, J., Zhao, G., Mao, X., Qin, H., & Zhao, Y. (2025c). Analysis of the carbody's lateral vibration characteristic of high-speed emus in turnout area. *Journal of Railway Science and Engineering*, *22*(1), 1–12.

Zhai, W., Stichel, S., & Ling, L. (2025). Train-track coupled dynamics problems in heavy-haul rail transportation. *Vehicle System Dynamics*, *63*(7), 1187–1240. doi: 10.1080/00423114.2025.2494834.

Zhang, H., Li, R., Ling, L., & Zhai, W. (2025). Dynamic analysis for the carbody chattering phenomenon induced by hunting instability of high-speed train. *Nonlinear Dynamics*, *113*(14), 17903–17932. doi: 10.1007/s11071-025-11144-w.

Zhao, Y., Xie, W., Li, H., Zhao, G., Yang, F., & Yang, S. (2026). A feature-enhanced rail-informer model for mapping vertical track irregularity to vehicle vertical acceleration. *Journal of the China Railway Society*, *48*(4), 1–12.

Corresponding author
Wanru Xie can be contacted at: xiewanru@rails.cn